Available online at www.sciencedirect.com
ScienceDirect
Atmospheric Environment 41 (2007) 7440–7461
ATMOSPHERIC ENVIRONMENT
www.elsevier.com/locate/atmosenv

Dilution and aerosol dynamics within a diesel car exhaust plume—CFD simulations of on-road measurement conditions

U. Uhrner[a,*], S. von Löwis[a], H. Vehkamäki[b], B. Wehner[a], S. Bräsel[a], M. Hermann[a], F. Stratmann[a], M. Kulmala[b], A. Wiedensohler[a]

[a]*Leibniz Institute for Tropospheric Research, 04318 Leipzig, Germany*
[b]*Department of Physical Sciences, University of Helsinki, 00014 Helsinki, Finland*

Received 7 June 2006; received in revised form 29 April 2007; accepted 24 May 2007

Abstract

Vehicle particle emissions are studied extensively because of their health effects, contribution to ambient PM levels and possible impact on climate. The aim of this work was to obtain a better understanding of secondary particle formation and growth in a diluting vehicle exhaust plume using 3-d information of simulations together with measurements. Detailed coupled computational fluid dynamics (CFD) and aerosol dynamics simulations have been conducted for H_2SO_4–H_2O and soot particles based on measurements within a vehicle exhaust plume under real conditions on public roads.

Turbulent diffusion of soot and nucleation particles is responsible for the measured decrease of number concentrations within the diesel car exhaust plume and decreases coagulation rates. Particle size distribution measurements at 0.45 and 0.9 m distance to the tailpipe indicate a consistent soot mode (particle diameter $D_p \sim 50$ nm) at variable operating conditions. Soot mode number concentrations reached up to $10^{13}\,m^{-3}$ depending on operating conditions and mixing.

For nucleation particles the simulations showed a strong sensitivity to the spatial dilution pattern, related cooling and exhaust $H_2SO_{4(g)}$. The highest simulated nucleation rates were about 0.05–0.1 m from the axis of the plume. The simulated particle number concentration pattern is in approximate accordance with measured concentrations, along the jet centreline and 0.45 and 0.9 m from the tailpipe. Although the test car was run with ultralow sulphur fuel, high nucleation particle ($D_p \leqslant 15$ nm) concentrations ($>10^{13}\,m^{-3}$) were measured under driving conditions of strong acceleration or the combination of high vehicle speed ($>140\,km\,h^{-1}$) and high engine rotational speed (>3800 revolutions per minute (rpm)).

Strong mixing and cooling caused rapid nucleation immediately behind the tailpipe, so that the highest particle number concentrations were recorded at a distance, $x = 0.45$ m behind the tailpipe. The simulated growth of H_2SO_4–H_2O nucleation particles was unrealistically low compared with measurements. The possible role of low and semi-volatile organic components on the growth processes is discussed. Simulations for simplified H_2SO_4–H_2O–octane–gasoil aerosol resulted in sufficient growth of nucleation particles.

Keywords: Aerosol dynamics modelling; Particle formation; Particle growth; Soot; Vehicle exhaust plume

1. Introduction

Adverse health effects such as lung cancer (e.g. Pope, 2000), cardiovascular disease (e.g. Peters

*Corresponding author. Now at Institute for Internal Combustion Engines and Thermodynamics, 8010 Graz, Austria. Tel.: +43 316 873 4588; fax: +43 316 873 8080.
E-mail address: uhrner@vkmb.tugraz.at (U. Uhrner).

1352-2310/$ - see front matter © 2007 Elsevier Ltd. All rights reserved.
doi:10.1016/j.atmosenv.2007.05.057

et al., 2001) bronchitis, asthma (Peters et al., 1997) and mutations (Somers et al., 2004) are associated with respirable particles emitted from vehicles. Ultrafine particles (defined as $D_p \leqslant 100$ nm) can deposit with high efficiency in the smallest vessels of the lungs. One major source of these ultrafine particles is vehicles. Furthermore, the influence of traffic-generated combustion particles on the earth radiation budget is controversially discussed (e.g. Jacobson, 2002; Penner et al., 2003).

According to health effect studies, the particle number concentration to which the individual is exposed is more important than their mass (e.g. Donaldson et al., 1998; Sydbom et al., 2001). The deposition efficiency of particles in the smallest vessels in the lung increases with decreasing particle size. For this reason and the fact that ultrafine particles contribute much to number and little to mass emissions, it is important to study the formation and fate of ultrafine particles in the exhaust plume of vehicles. Thereby, various processes such as dispersion, coagulation, deposition, new particle formation and growth must be assessed.

Diesel engines primarily emit aerosol precursor gases such as SO_2, SO_3, H_2SO_4, NO_x, H_2O, low and semi-volatile organic species as well as soot particles. At the engine exhaust port, soot particles are fractal-like agglomerates, which undergo complex processes like compaction and condensation of low and semi-volatile organics, which result in higher density and less irregular shape until they leave the exhaust pipe. Exhaust size distribution measurements made at various diesel cars are similar for comparable operation conditions unless nucleation occurs. They exhibit a consistent soot mode at a particle mobility diameter of 50–100 nm (e.g. Harris and Maricq, 2001). Dependent on fuel composition, engine operating conditions, exhaust aftertreatment, exhaust dilution and sampling methods, the size distribution can exhibit a second highly variable nucleation mode with diameters from 10 to 20 nm (e.g. Maricq et al., 2002; Vogt et al., 2003; Giechaskiel et al., 2005). Earlier works all undertaken on heavy-duty diesel engines resulted in qualitatively similar results (Baumgard and Johnson, 1996; Khalek et al., 1999; Shi and Harrison, 1999). Nucleation particles can dominate the number concentration of ultrafine particles. In contrast to soot mode particles, there is only limited information available on the chemical composition of nucleation mode particles. Volatility tandem DMA (VTDMA) measurements suggest that most of these particles are semi-volatile and do not have a solid core (Scheer et al., 2005; Maricq et al., 2002). Highway roadside measurements by Wehner et al. (2004) showed a bi-modal distribution with a volatile nucleation mode and a small volatile fraction of soot mode particles. The nucleation mode is thought to originate from sulphuric acid and/or semi-volatile organic gases that nucleate and condense during exhaust dilution. There is strong evidence that nucleation particles in vehicle exhaust may be formed by binary homogenous nucleation of sulphuric acid and water. In several studies, high particle number concentrations were related to high fuel sulphur content and exhaust aftertreatment such as the use of oxidation catalysts (e.g. Baumgard and Johnson, 1996; Maricq et al., 2002; Vogt et al., 2003). Oxidation catalysts remove a large fraction of hydrocarbons and boost SO_2 to SO_3 oxidation. SO_3 then rapidly reacts with exhaust H_2O forming sulphuric acid. Further suggested particle formation mechanisms are homogeneous ternary nucleation of H_2SO_4, NH_3 and H_2O (Shi and Harrison, 1999) and heterogeneous ion-induced nucleation (Yu, 2001). However, the relevance of these mechanisms is still not clear. Organic compounds are considered to control the growth of nucleation particles in diesel exhaust plumes (Khalek et al., 2000; Tobias et al., 2001; Sakurai et al., 2003).

A key factor for nucleation is the dilution of exhaust gases. During dilution, aerosol precursor gases cool and the saturation ratios of semi-volatile species go through a maximum, which may lead to nucleation and/or condensation. Engine test-bed investigations indicate that the occurrence of nucleation particles strongly depends on dilution ratio, residence time, dilution temperature and relative humidity. However, Maricq et al. (2002) and Vogt et al. (2003) encountered difficulties when comparing laboratory data to either wind tunnel or on-road (e.g. chasing) measurements. Giechaskiel et al. (2005) concluded that vehicle exhaust nucleation mode particles can be at least qualitatively reproduced in the lab.

In principle, a coupled CFD-aerosol model approach enables to account for all relevant concurrent processes in the exhaust plume, including turbulent diffusion. Moreover, 3-d pattern of all parameters of interest are calculated and can be used for validation with point measurements and further interpretation due to the 3-d information.

However, there have been very limited investigations on the simulation of exhaust gas and particle dispersion so far. Kim et al. (2002) found very good agreement with CFD CO_2 dispersion simulations compared against measurements for a heavy tractor (truck without trailer) placed in an aircraft wind tunnel. In a further study (Kim et al., 2001), based on the dilution ratio of CO_2, nucleation, condensation and coagulation for H_2SO_4–H_2O aerosol was calculated with a non-coupled aerosol model in the plume. A good agreement between simulated and measured size distribution was obtained. Carbonaceous particle emissions were not considered.

Jiang et al. (2005) showed the impact of vehicle speed on soot particle size distributions based on CFD calculated CO_2 dilution for the simulation of dilution and coagulation on five streamlines. They found that increasing vehicle speed caused more rapid dilution and inhibited coagulation.

In this project, the transformation processes under turbulent diffusion within the exhaust plume in the wake of a passenger vehicle were studied for typical atmospheric and on-road conditions. Particle and trace gas measurements as well as temperature and flow velocity measurements were made under real conditions on public roads. The motivation for this combined approach by measurements and simulations was to evaluate conditions leading to particle formation within the exhaust plume and to gain insight into several important simultaneous processes affecting particle formation such as: cooling of exhaust gas upon turbulent dilution, dilution of particles and precursor gases with ambient air, coagulation and condensation. Therefore, the dilution and aerosol dynamics within and around the exhaust plume were modelled using computational fluid dynamics software (FLUENT 6, www.fluent.com) together with the add-on aerosol model FPM (Fine Particle Model, www.particle-dynamics.de). The FPM, together with FLUENT, represents a full Eulerian solution of the particle general dynamics equation. Therefore, in contrast to previous studies where particle dynamics was only computed along selected streamlines, use of the FPM permitted a fully coupled Eulerian/Eulerian simulation of the aerosol dynamics on all grid cells.

In this work, the following key factors that influence the formation and growth of new particles in the exhaust plume were considered using 3-d numerical simulations and point measurements: sulphuric acid flux, engine operating conditions, the turbulent dilution of the exhaust flow, temperature and humidity. Emitted soot mode particles influence on nucleation by acting as condensational sink for sulphuric acid during dilution. The impact of low and semi-volatile hydrocarbons on growth was estimated.

2. General approach

The test car and vehicle modelled was a European 2003 estate car, which is used as a common staff car at the Institute for Tropospheric Research (IfT) in Leipzig. The car has a 2.0 l DTI 16 V 74 kW (100 hp) diesel engine. The vehicle is equipped with an oxidation catalyst, but has no particle filter. The car attained the Euro 3 exhaust emission standard. The test car was run with low sulphur standard fuels containing $\sim$7 ppm_m sulphur content. The test car had been operated for 27,500 km before we did our measurements.

In order to describe the interaction of flow, dilution and aerosol dynamics behind the exhaust pipe in the wake of the car FLUENT CFD-software and the FPM were used to compute 3-d particle concentrations.

Due to computational limits, only steady-state operating conditions were examined and the focus of the modelling efforts was placed on the exhaust region whereas the body of the car was simplified. Measurements have been used in particular for the verification of model results concerning nucleation and for certain boundary conditions like the determination of soot particle emissions, exhaust out temperature, gas composition and flow rate.

2.1. Measurements

Here, measurement results recorded on 13 October 2004 are presented for comparison with model results. The measurement devices and data acquisition system were placed inside the car and the inlet and sensor system was mounted on a bicycle rack (see Fig. 1). The following measurements were made within the exhaust plume: particle size distribution with an Scanning Mobility Particle Sizer (SMPS) system, CO_2 and NO_x with a Multigas Emission Analyser (CLIR 2M Ansyco), relative humidity (RH) with Vaisala sensors, temperature (T) with thermocouples and Vaisala sensors, and velocity measurements with a Prandtl Pitot tube. The measurement range and time resolution of the instruments are listed in Table 1. The spatial range within the exhaust plume was confined to

Fig. 1. Test car with mounted inlet and sensor system.

a maximum of $x = 1$ m.[1] For operating conditions ranging up to 148 km h^{-1} and 4000 rpm, the minimum centreline distance was set to 0.45 m in order to avoid temperature damage to the Vaisala sensors, exceeding the maximum counting frequency of the SMPS system and to prevent condensation and new particle formation within the sampling system. One thermocouple was placed at the tailpipe exit to monitor the undiluted exhaust gas temperature. The sampling inlet was mounted at either $x = 0.45$ or 0.9 m. The temperature and humidity sensors were mounted within a few cm distances to the inlets for the aerosol, gas and flow measurement systems.

Measurements concerning the vehicle operating conditions such as vehicle speed, rpm, and air mass flow were recorded with an Online Board Diagnosis (OBD) tool. The test legs were driven on the German motorway A38 between two different motorway exits. Further details about the measurements can be found in von Löwis (2006).

2.2. CFD model set-up and verification

FLUENT was used to solve the 3-d Reynolds averaged equations for flow, pressure, turbulence parameters and the gas-phase concentration distribution (FLUENT 6 User's Guide, 2001). The "two equation" standard k–ε model based on the isotropic eddy viscosity assumption was chosen to predict the Reynolds stresses.

[1]For safety reasons, in Germany additional load and mountings are only allowed up to a distance 1 m behind the car.

Because mixing behind the exhaust pipe of the vehicle was of primary interest in this study, the CFD model was not intended to be a detailed aerodynamic vehicle simulation. Due to CPU time and memory limitations, we did not attempt to fully resolve the vehicle geometry or the fluid boundary layers surrounding the vehicle. These are expected to have little effect on exhaust mixing in the wake of the test car. Based on a technical drawing of the estate car available on the manufacturer website, a simplified model geometry was created with GAMBIT (www.fluent.com) and placed in a model domain 20 m high, 20 m wide and 50 m long, essentially a computational wind tunnel (see Fig. 2). The numerical solution of the equations used an irregular grid that follows the shape of the car. In the near-exhaust region, the finest mesh resolution was created, decreasing exponentially in x-, y- and z-directions towards the outer boundaries of the model domain. Approximately 260,000 tetrahedral grid cells were utilised. Gradient adaptation was applied to further improve the mesh quality. Second-order upwind discretisation schemes were used for the numerical solution to increase the accuracy and reduce numerical diffusion.

The movement of the car was solved in the relative velocity frame of reference, i.e., no slip at the car surfaces. The ambient air velocity was set equal to the car velocity but opposite in direction (see Fig. 2). Symmetric boundary conditions (zero gradient normal to boundary) were applied to the top and the sidewalls approximating free stream conditions. The bottom of the domain, representing the road was defined as "moving wall" (corresponding to vehicle speed) with a no-slip condition. The left side of the box shown in Fig. 2 was defined as velocity inlet. The right side of the box is the outflow region and was defined as pressure outlet. Here, the setting of boundary values concerning chemical composition and particle properties is only relevant in case of backflow at the first iterations. The end of the exhaust pipe, 52 mm in diameter, was specified as mass flow inlet (into the surrounding continuum) with an exhaust gas mass flow rate (in kg s^{-1}) and species mass fractions, respectively. The exhaust gas flow rate was assessed from our OBD data for the air mass flow. The exhaust gas velocity was calculated by the CFD model based on the given exhaust gas flow rate, temperature and diameter. The exhaust gas composition and fuel/air ratio were chosen following motor test bench measurements and fuel sulphur content. Various

Table 1
Measurement devices and their range and time resolution

Device	Range	Resolution	Parameter
SMPS	7–400 nm	1.5 s, 90 s per scan	Number size distribution
Emission analyser	0–5 vol%	15 s	CO_2
	0–1000 ppm_v	10 s	NO_x
Vaisala sensor	0–100%	5 s	RH
	−40–180 °C	5 s	T
Thermocouple	−25–550 °C	10 ms	T
Prandtl Pitot tube	0–40 m s^{-1}	10 ms	Velocity
OBD	Vehicle dependent	1 s	Car speed, rpm, air mass flow

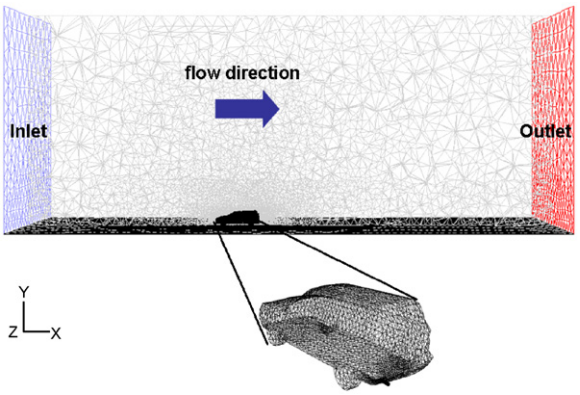

Fig. 2. Test car geometry and computational domain for the CFD simulations. The dimensions of the car are 4288 mm length, 1709 mm width and 1510 mm height. The inlet is located to the left (purple mesh, the outlet to the right (red mesh), and the grey mesh is a cross-section in the exhaust pipe plane.

studies on atmospheric nucleation showed that binary homogeneous H_2SO_4–H_2O nucleation is very sensitive to $H_2SO_{4(g)}$ concentrations (e.g. Kulmala et al., 1998; Vehkamäki et al., 2003; Berndt et al., 2005). Exhaust nucleation particle concentrations are very sensitive to fuel sulphur content (e.g. Baumgard and Johnson, 1996; Kittelson, 1998; Khalek et al., 1999; Shi and Harrison, 1999; Vogt et al., 2003) and thus $H_2SO_{4(g)}$ is considered to be important in particle formation in an exhaust plume. To the author's knowledge, no exhaust plume $H_2SO_{4(g)}$ measurements have been published yet. Hence, based on particle composition measurements taken from a heavy duty diesel engine, Baumgard and Johnson (1996) estimated the net fuel sulphur to sulphate conversion to be 4%. Within the DECSE (1999) (Diesel Emission Control—Sulfur Effects Program) program, the impact of fuel sulphur content and the impact of a diesel oxidation catalyst on particulate matter emissions were investigated for two heavy duty diesel engines. Engine sulphur conversion rates were in the range of 1–3% and an increase proportional to the amount of fuel sulphur was found. However, post catalyst conversion rates increased with increasing exhaust temperatures (up to 518 °C at the catalyst), and reached a maximum of 15%. In this work, $H_2SO_{4(g)}$ concentration fluxes are therefore prescribed as a boundary condition at the end of the exhaust pipe. The exhaust $H_2SO_{4(g)}$ mass fraction, that can be attributed to the fuel sulphur content, can be calculated as

$$H_2SO_{4(g)} = \frac{F/A \times \mathrm{fsc} \times \mathrm{cr} \times w_{SA}/w_S}{F/A + 1}, \quad (1)$$

where F/A is the fuel/air ratio, fsc the fuel sulphur content, cr the SO_2 to SO_3 conversion rate and w_{SA} and w_S denote the molar weights of sulphuric acid and the sulphur, respectively. Hence, the exhaust $H_2SO_{4(g)}$ concentration flux is the product of the $H_2SO_{4(g)}$ mass fraction and the total exhaust mass flow rate (mfr). Sulphur in the lube oil and desorption from the exhaust line may increase the $H_2SO_{4(g)}$ content calculated in Eq. (1). However, it is difficult to estimate the exact contribution of these two sources as a boundary condition. The effect of lube oil and desorption on particle formation is further elaborated when results on particle nucleation are presented.

Boundary conditions for the velocity inlet and exhaust pipe used in this study are shown in Tables 2 and 3.

To test the CFD model, simulation results were compared to time-averaged measurements of CO_2 concentrations, temperature and relative humidity inside the dispersing plume taken from "real world" conditions on motorways (Figs. 3–6). The boundary conditions were chosen as shown in Table 2, and the exhaust gas composition was assumed to be that

Table 2
Boundary conditions for CFD test runs, mfr denotes the mass flow rate

	V	T	H_2O	CO_2
Velocity inlet	120 km h^{-1} measured	283 K $T_{ambient}$	65% $RH_{ambient}$	570 ppm_m
Exhaust pipe	Calculated from mfr (0.055 kg s^{-1})	480 K measured	Calc. flux (mfr 6 wt%)	Calc. flux (mfr 14 wt%)

Table 3
Boundary conditions for simulations including nucleation and condensation, mfr denotes the mass flow rate

	V	T	H_2O	CO_2
Velocity inlet	148 km h^{-1} measured	300 K $T_{ambient}$	65% $RH_{ambient}$	570 ppm_m
Exhaust pipe	Calculated from mfr (0.1 kg s^{-1})	550 K measured	Calc. flux (mfr 6 wt%)	Calc. flux (mfr 14 wt%)

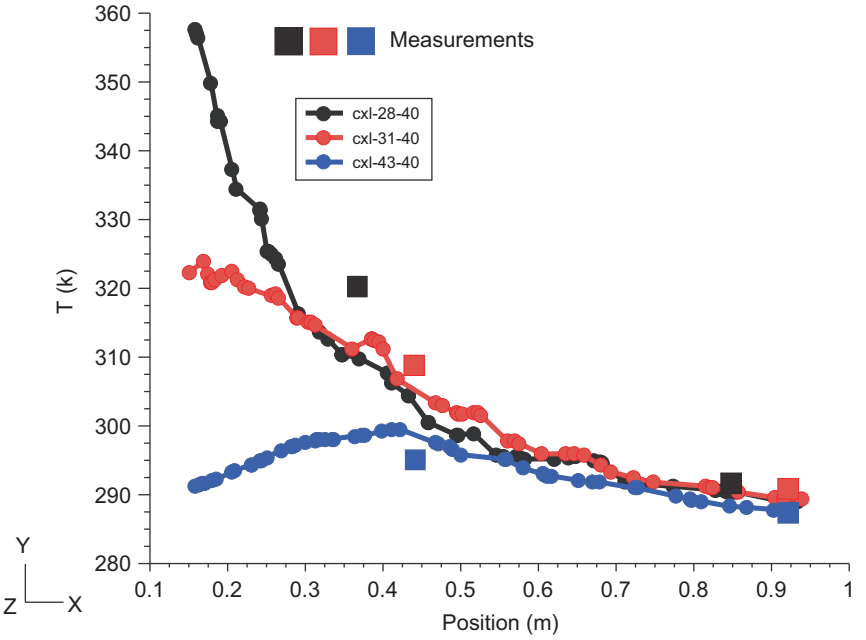

Fig. 3. Simulated temperature (lines) and measured values (squares). The diagram shows the position in the x-direction and the legend indicates the height above ground (0.28, 0.31 and 0.43 m). The variance at the measurement point at $x = 0.45$ m is 3.7 K and at $x = 0.9$ m is 1.3 K.

measured during motor test bench measurements at $F/A = 0.037$. In addition, simulations with grid refinement and coarsening in the exhaust plume region were performed. The simulation results showed no significant impact of resolution on the concentration fields.

The CFD model results for T, RH, flow velocity and CO_2 concentration were compared to measurements at various locations within the exhaust plume. A fair agreement for 120 km h^{-1} was obtained for the simulated exhaust plume temperature (6 measurement points), CO_2 (2 points), relative humidity (2 points) and x-velocity (2 points). The results are shown in Figs. 3–6.

2.3. Aerosol model

The FPM describes the dynamic changes of the particle size distribution and chemical composition, coupled with fluid flow including heat and mass transfer. Processes such as turbulent particle diffusion, particle formation, condensation, evaporation,

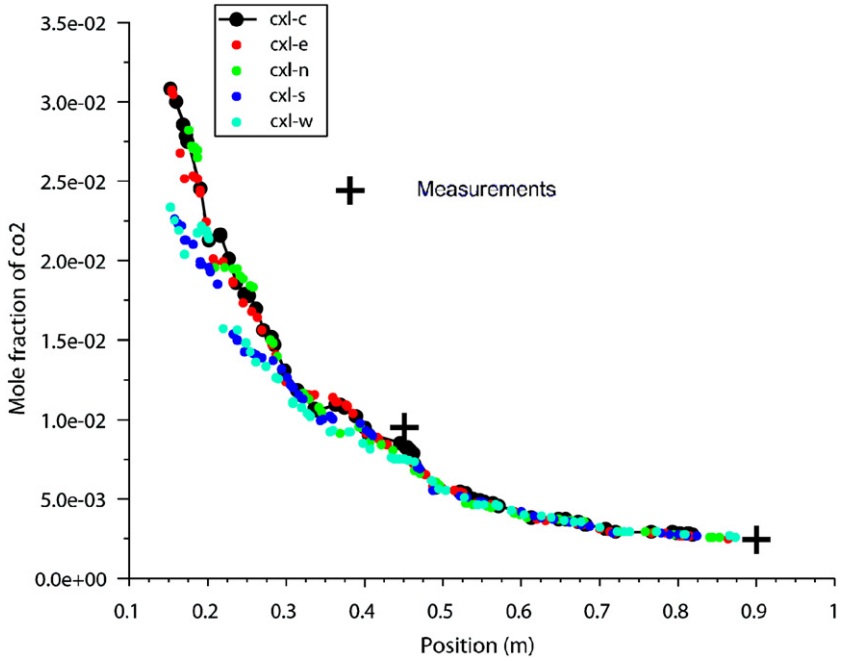

Fig. 4. Simulated CO_2 (circles) and measurements (plus signs) on and around the exhaust plume centreline, cxl-c indicates the centreline, cxl-w is shifted 2 cm to the left, cxl-e is shifted 2 cm to the right, cxl-n is shifted 2 cm upward and cxl-s is shifted 2 cm downward. The variance of CO_2 at the measurement point at $x = 0.45$ m is 900 ppm and at $x = 0.9$ m is 250 ppm.

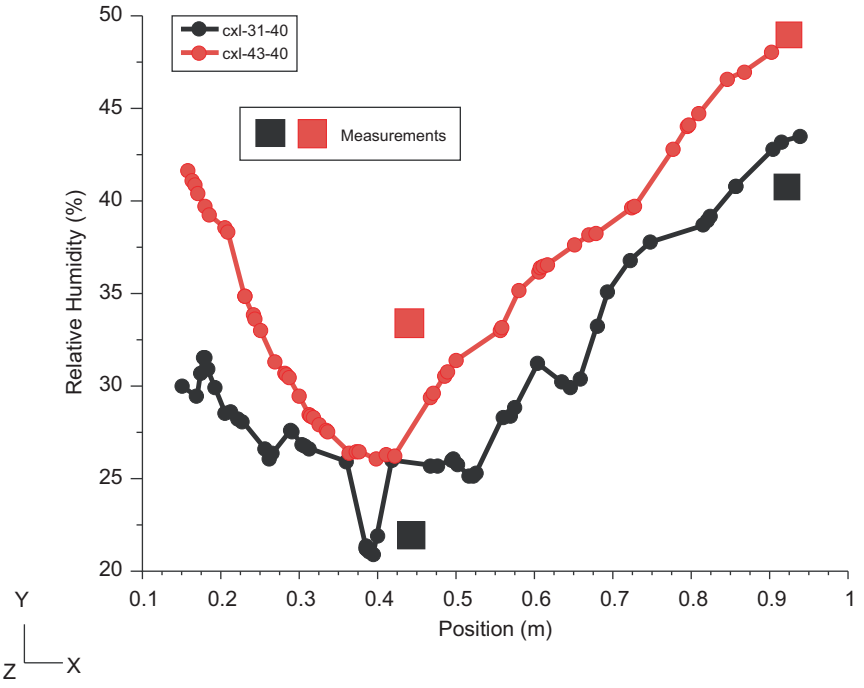

Fig. 5. Simulated (lines) and measured RH (squares). The Vaisala sensors were located at 0.31 and 0.43 m above the road. The variance at the measurement point at $x = 0.45$ m is 2% and at $x = 0.9$ m is 4%.

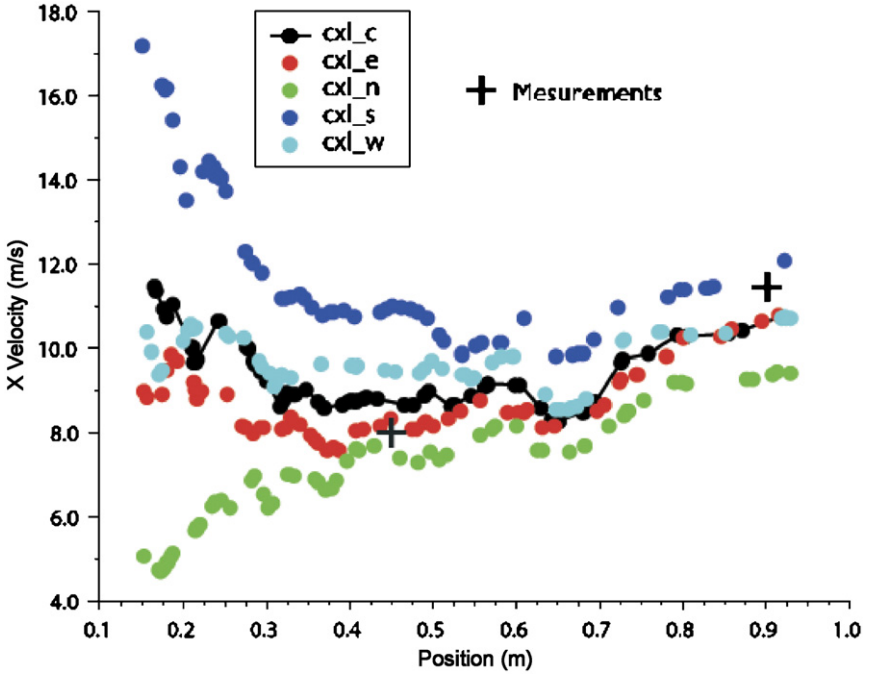

Fig. 6. Simulated and measured x-velocity (plus signs). The variance at the measurement point at $x = 0.45$ m is 3.7 m s^{-1} and at $x = 0.9$ m, 1.9 m s^{-1}.

coagulation and deposition processes are computed utilising a Eulerian/Eulerian solution technique. The FPM is used within the framework of FLUENT 6. It utilises the method of moments together with the modal assumption. It is assumed that the particle size distribution can be represented as superposition of an arbitrary number of modes (Whitby, 1978). Prognostic variables are the moments $M_{k,i}$ of the modes i used to represent the particle size distribution $n(m_p)\,dm_p$ depending on particle mass m_p:

$$M_{k,i} = \int_0^\infty m_p^k n_i(m_p)\,dm_p. \quad (2)$$

For the closure of the moment equations, lognormal size distributions are assumed for each mode i. The modes are composed of internally mixed particles, which consist of multiple immiscible phases. Each phase can be composed of multiple chemical species.

In order to simulate aerosol dynamics within the exhaust plume, at first two phases soot (solid) and H_2SO_4–H_2O (liquid) were considered and the FPM was extended by growth and nucleation thermodynamics by means of user defined functions. Additionally, the effect of volatile hydrocarbons on particle growth was assessed.

The underlying assumptions for the model are:

(i) nucleation mode particles may be formed by H_2SO_4–H_2O nucleation and can further grow by condensation or coagulation;
(ii) soot mode particles are directly emitted from the exhaust and can grow by coagulation and condensation of H_2SO_4 and H_2O assuming a core mantle spherical particle shape;
(iii) to estimate the contributions of simplified organics a third non-interacting phase consisting of octane and gas oil was added.

To keep the computational burden low and to avoid numerical instabilities, the following assumptions and approximations were used:

- for small particles and low relative humidity water condensation and evaporation are very fast processes (Wilck, 1998); hence, the particle water content was calculated in equilibrium to reduce the numerical stiffness due to water condensation/evaporation;
- the geometric standard deviation, σ, for both modes was kept constant, i.e. $\sigma = 1.5$ for the nucleation mode and $\sigma = 1.8$ for the soot-mode based on our measurement results.

For H_2SO_4–H_2O growth processes, the thermodynamics from Zeleznik (1991) was implemented by means of user-defined functions. The calculation of the H_2SO_4 and H_2O mole fractions must be done iteratively when the equilibrium approach for water is utilised. To save CPU time parameterisations have been developed and are described in the Appendix. The parameterised binary nucleation rate for high temperatures (300–400 K) from Vehkamäki et al. (2003) was used. The basic equations of the FPM can be found in Wilck and Stratmann (1997).

2.4. Parameter settings and boundary conditions for simulations

Due to the large computational efforts, we focus on two motorway operating conditions:

(a) 120 km h^{-1}/5th gear/2600 rpm,
(b) 148 km h^{-1}/4th gear/4000 rpm.

The measured size distribution showed a dominant soot mode for condition (a), whereas for (b) large dominant concentrations of nucleation particles were recorded. The simulations are based on the assumption that number and size of soot mode particles are related to operating conditions and the type and size of the diesel engine, whereas nucleation particles form within the vehicle exhaust plume, and hence are dependent on ambient conditions as well.

For condition (a), only diffusion and coagulation within the exhaust plume were considered. A bimodal size distribution consisting of a soot mode with $d_{gn} = 50$ nm, $N = 10^4$ cm^{-3}, $\sigma = 1.6$ and a background accumulation mode with $d_{gn} = 120$ nm, $N = 2.5 \times 10^3$ cm^{-3}, $\sigma = 1.8$ was used. Temperature and RH were set to ambient conditions. An exhaust soot mode particle flux was set as a boundary condition. This soot mode emission factor was determined by running a few simulations with varied soot mode particle fluxes in order to obtain the best match with averaged measurements taken at $x = 0.45$ and at 0.9 m (see Figs. 7 and 8). The effect of particle deposition on surfaces such as road and car body is considered to be small and therefore not accounted.

For condition (b), a soot mode as described for condition (a) and a nucleation mode were used in the simulations. Number and size of the nucleation mode were computed by the FPM.

The exhaust $H_2SO_{4(g)}$ flow rate was set to 9×10^{-7} and 3×10^{-7} mol s^{-1}, respectively. The first

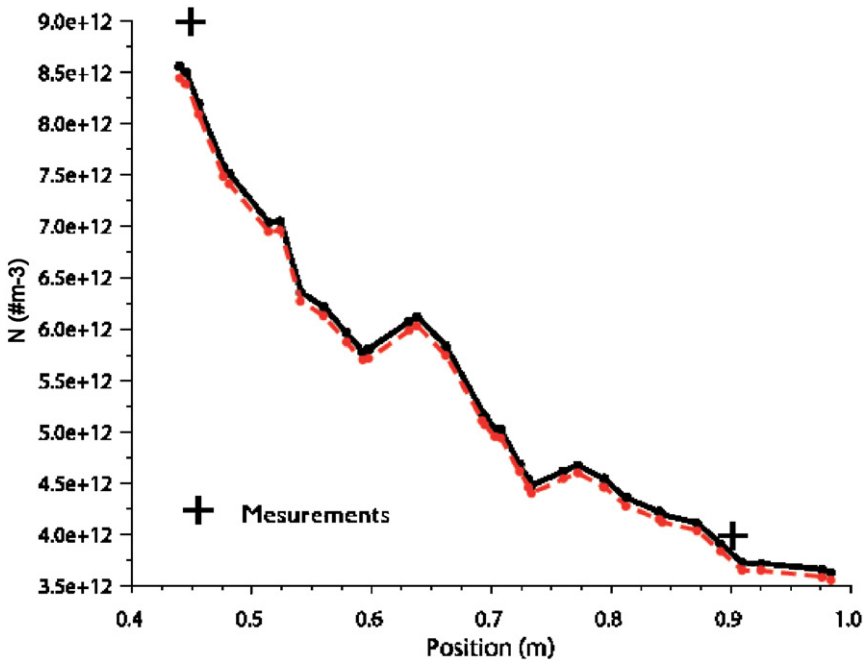

Fig. 7. Decrease in soot mode number concentration (#m^{-3}) on the exhaust centreline for simulations with (red curve) and without coagulation (black curve). The plus signs indicate measured values. Typical conditions for 120 km h^{-1}/2600 rpm were chosen for these simulations. The ambient size distribution was bi-modal (cf. Table 6) and the size distribution of the exhaust was unimodal.

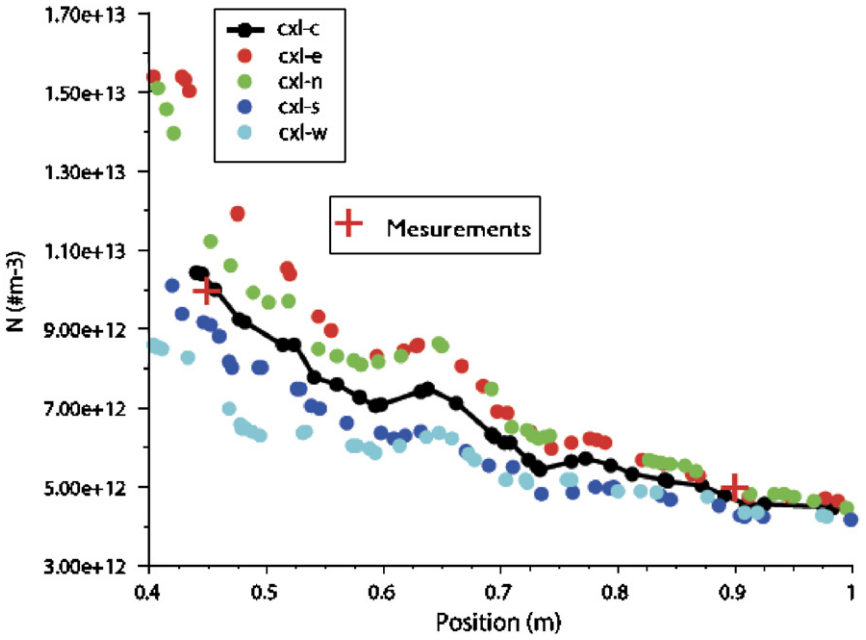

Fig. 8. Simulated soot mode number concentrations ($\#m^{-3}$) on and around the exhaust plume centreline (148 km h^{-1}/4000 rpm). The plus signs indicate measured values.

flux corresponds according to Eq. (1) to a fuel sulphur content of 350 ppm_m and a conversion rate of 0.03 or a lower fuel sulphur content of, e.g. 10 ppm_m at a conversion rate of 1. Consequently, a flux of 3×10^{-7} mol s^{-1} would correspond to 10 ppm_m sulphur content and a conversion rate of 0.33. Currently, the standard for diesel sulphur content in the EU is 50 ppm_m. The boundary conditions are presented in Table 3, F/A was set to 0.034.

The temperature range of the parameterisations used is from 300 to 400 K. During the experiments ambient temperatures ranged from 278 to 285 K and exhaust gas temperatures reached up to 550 K. Therefore, a direct comparison of modelled results versus measurements involves extrapolating the temperature range of the parameterisations used for H_2SO_4–H_2O nucleation and growth at temperatures <300 K. For temperatures >400 K, the nucleation and particle growth rates were assumed to be 0.

3. Experimental results

Measured time series for the test-car velocity, revolutions per minute (rpm) and the aerosol number size distributions are shown in Fig. 9.

The size distributions shown in Fig. 9 exhibit a consistent maximum in particle number concentration of $\sim 10^{13}$ m^{-3} peaking at about 50 nm, the so-called soot mode. At low to medium load driving conditions nucleation mode particle concentrations are low. During strong acceleration or at constant speeds >140 km h^{-1} and at high rpm, nucleation mode particle concentrations up to $\sim 5 \times 10^{13}$ m^{-3} were measured within the exhaust plume. These conditions are characterised by the highest exhaust plume temperature and largest NO_x concentrations (see Table 4).

Averaged modal parameters derived from size distribution measurements (five up and down SMPS scans) at $x = 0.45$ and 0.9 m are shown in Table 5 to provide a brief overview of the measurements. The fitted size distributions showed generally a unimodal structure, but under high engine load conditions they showed a bi-modal structure. The soot mode geometric mean diameter was around 50 nm, whereas σ ranges from 1.6 to 1.9. This is in accordance with chassis dynamometer and chasing experiment data for a comparable diesel engine presented by Vogt et al. (2003). The number concentration ratio of soot-mode particles measured at $x = 0.45$ and 0.9 m was about 2:1. At 120 km h^{-1}, no significant concentrations of nucleation mode particles were measured. At 148 km h^{-1} and

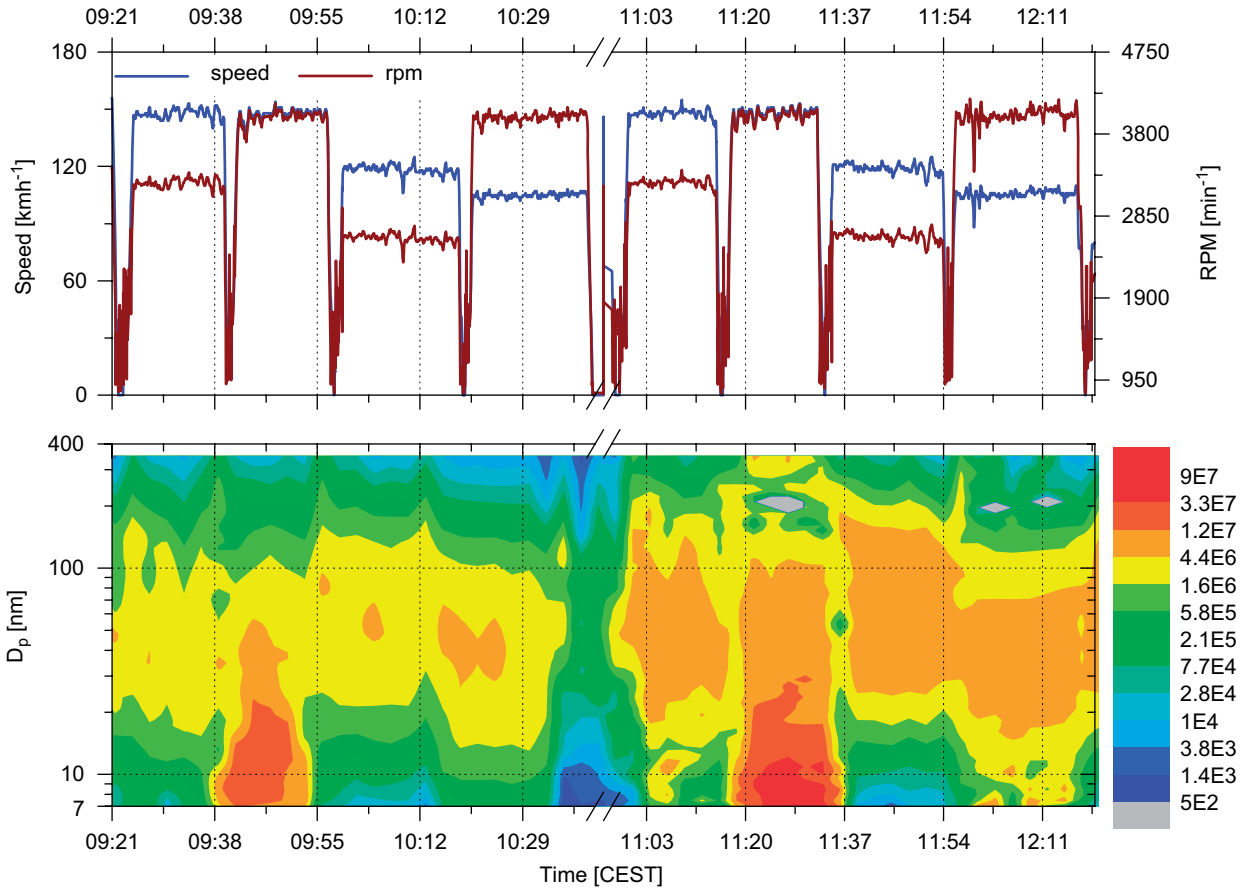

Fig. 9. Measured vehicle speed and rpm (top), evolution of the size distribution on 13 October 2004 (bottom). Note, the unit for $dN/d\log d_p$ is given in #cm^{-3}, the inlet and sensor system was positioned at $x = 0.9$ m from 9:20 to 10:40 and thereafter at $x = 0.45$ m.

Table 4
Data sampled at $x = 0.45$ m (upper values) and $x = 0.9$ m (lower values)

V (km h^{-1})	rpm (min^{-1})	Gear engaged	T (K)	CO_2 (ppm$_v$)	NO_x (ppm$_v$)
120	2600	5	318	9500	22
			290	2500	5
148	3200	5	335	11300	76
			298	4078	28
148	4000	4	342	10400	124
			310	5500	62

Mean values were obtained averaging over 10 scans.

3200 rpm soot mode particles dominate, but nucleation mode particle concentrations as high as $\sim 10^{12}$ m^{-3} were recorded at 0.45 m. At 0.9 m, there were no indications of nucleation mode particles. The reason for this could be the impact of turbulent diffusion and/or concurrent rapid growth to larger sizes. At 148 km h^{-1}/4000 rpm, nucleation mode particles clearly dominated at both sampling points. This gives some indication that the soot mode particle concentrations are reduced at the larger distance by dilution and/or coagulation, whereas nucleation mode particles may undergo dilution, self-coagulation, coagulation with soot mode particles and possibly still further formation to the larger distance. Simulations were used to evaluate the relative importance of these interacting processes.

4. Simulation results and discussion

The aim of this modelling work was to accurately describe dilution and coagulation of soot mode particles and then to consider all relevant processes leading to new particle formation using 3-d numerical simulations.

Table 5
PM emissions: data sampled at $x = 0.45$ m (upper values) and $x = 0.9$ m (lower values)

V (km h^{-1})	rpm (min^{-1})	N_{nuc} (m^{-3})	$d_{g\text{-}nuc}$ (nm)	σ_{nuc}	N_{soot} (m^{-3})	$d_{g\text{-}soot}$ (nm)	σ_{soot}
120	2600	–	–	–	9e12	45	1.6
		–	–	–	4e12	51	1.6
148	3200	1e12	10	1.3	8e12	48	1.9
		–	–	–	3e12	52	1.7
148	4000	5e13	6	1.9	1e13	44	1.8
		2e13	11	1.5	5e12	45	1.6

Mean values were obtained by fitting SMPS size distributions to a log-normal distribution from 10 scans.

Measurements or simulations of engine and exhaust aftertreatment-related effects and processes are beyond the scope of this work. Hence, exhaust gas flow and composition were prescribed. First, dilution and coagulation of a uni-modal exhaust soot mode distribution will be examined before additionally simulated growth and nucleation will be analysed.

4.1. Dilution and coagulation of soot mode particles

An exhaust soot-mode emission factor of 7×10^{12} s^{-1} (2.1×10^{14} km^{-1}) was determined by fitting soot-mode number concentrations measurements to simulations at $x = 0.45$ and 0.9 m for simulations representing operating conditions of 120 km h^{-1} and 2600 rpm (see Fig. 7).

In order to asses the impact of coagulation within the exhaust plume, two cases were calculated considering (i) only particle diffusion and (ii) particle diffusion and coagulation. The boundary conditions were the same in both cases (Table 2). The background particle number concentrations represent the urban background of Leipzig (Wehner, 2000) and are shown in Table 6. Fig. 7 shows that the impact of coagulation in the near plume region is negligible and the decrease in N_{soot} within 1 m distance is primarily due to turbulent dilution. The reason for the minor impact of coagulation is the short residence time (<0.1 s) of particles in the near-exhaust region as opposed to rapid dilution.

Exhaust jet emissions do not penetrate to a large extent in the recirculation zone higher up in the wake of the vehicle (see Fig. 10) where high residence times can lead to a large effect of coagulation in reducing particle concentrations. Jiang et al. (2005) obtained similar results for the exhaust plume simulations of a slowly (up to 32 km h^{-1}) moving truck.

Table 6
PM background values

	N (m^{-3})	d_{gn} (nm)	σ
Ait-mode	1e10	50	1.8
Acc-mode	2.5e9	120	1.9

4.2. Simulations with condensation and nucleation

The aim of the following simulations was to study homogeneous H_2SO_4–H_2O nucleation within the wake of the car and to attain a 3-d representation of nucleation particle concentrations and other relevant parameters. These fields were used to analyse secondary exhaust particle formation and further interpretation of our measurements. As described in the previous section, the impact of an accumulation mode to coagulation scavenging is negligible. Assuming a soot mode particle concentration of 10^{12} m^{-3} with 50 nm mean diameter within the exhaust plume, and a background accumulation mode concentration of 2.5×10^{9} m^{-3} with 120 nm diameter, the particle surface area concentration of soot mode particles is roughly two orders of magnitude larger than the accumulation mode concentrations. Hence, the impact of a background accumulation mode acting as a condensational sink within the test-car exhaust plume should be negligible as a first approximation. In the following simulations, focusing on nucleation and condensation a bi-modal size distribution was used to reduce the computational burden compared with tri-modal simulations.

The soot-mode emission factor was determined to 1×10^{13} s^{-1} (2.6×10^{14} km^{-1}) for 148 km h^{-1} and 4000 rpm (see Fig. 8).

As shown in Fig. 11, a sulphuric acid flux of 9×10^{-7} mol s^{-1} results in $\sim 10^{13}$ m^{-3} nucleation

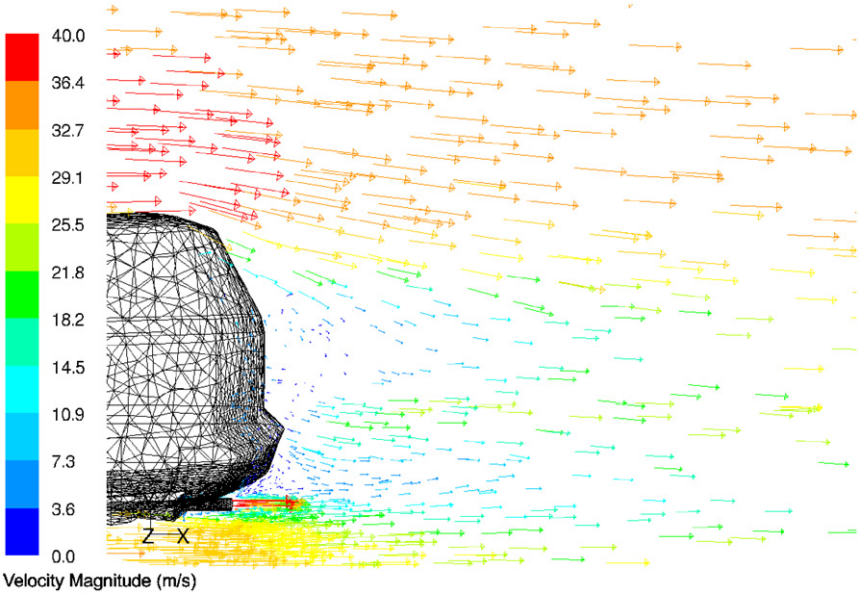

Fig. 10. Cross-sections for simulated velocity vectors in the exhaust pipe plane (120 km h^{-1}/2600 rpm). The colours indicate the velocity magnitude.

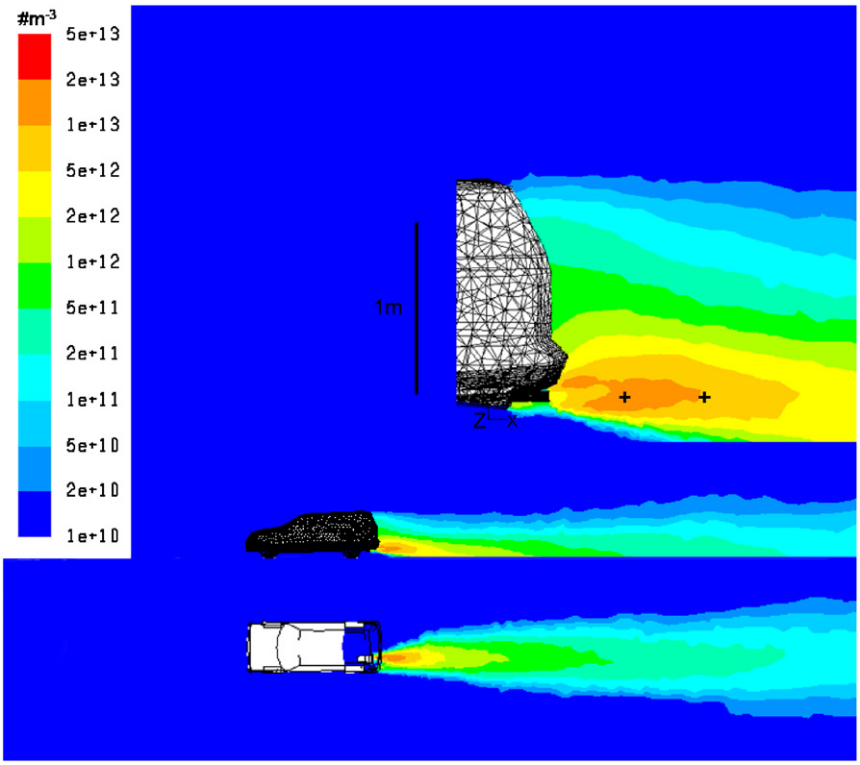

Fig. 11. Cross-sections for simulated nucleation mode number concentration (#m^{-3}) in the exhaust pipe plane (top and side view as well as close-up for near-exhaust plume region). Simulation parameters were $V = 148$ km h^{-1}, 4000 rpm, $T_{ambient} = 300$ K, $RH_{ambient} = 65\%$, and 0.09 ppm_m s^{-1} exhaust-$H_2SO_{4(g)}$. The plus signs indicate the position of the inlet and sensor system, measured values were at $x = 0.45$ m, 5×10^{13} #m^{-3} and at $x = 0.9$ m, 2×10^{13} #m^{-3}.

particles in the near-exhaust region (at $x = 0.45$ m, 1.5×10^{13} m^{-3} and at $x = 0.9$ m, 0.9×10^{13} m^{-3}. A factor of 3 lower sulphuric acid flux results in a significantly decreased nucleation rate and predicted nucleation particle concentrations are slightly higher than the background number concentrations, i.e. $\sim 10^{11}$ m^{-3}(not shown).

The simulated number concentrations are highest close to the plume axis at about $x = 0.4$ m. This agrees with the measurements, where the highest concentrations were consistently found at $x = 0.45$ m rather than at $x = 0.9$ m.

The highest nucleation rates are found in those areas where the gradients of H_2SO_4, T and RH are strongest (see Fig. 12(a)–(d)) and dilution gradients as indicated by the CO_2 dilution ratio (Fig. 12(d)) is highest.

Although ambient temperature and to a lesser extent RH were set significantly different from the measurement conditions, the sulphuric acid

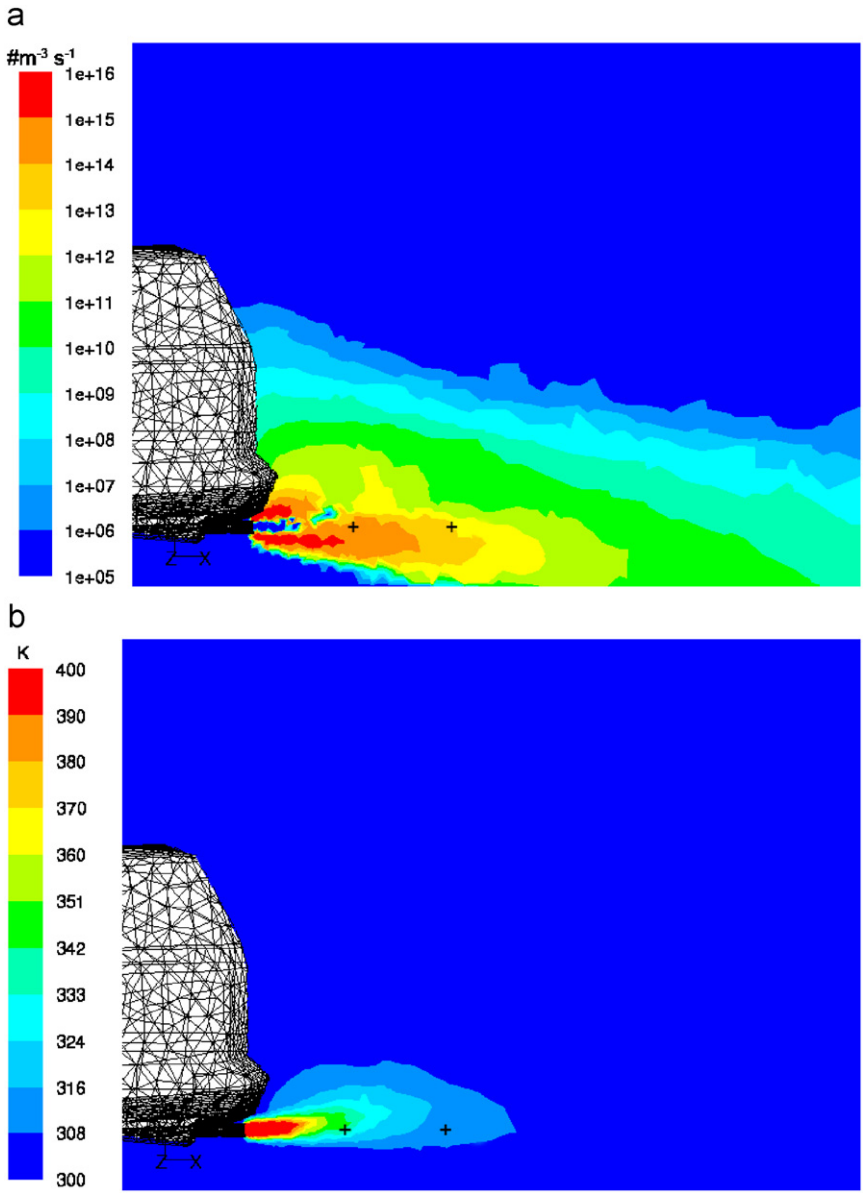

Fig. 12. Cross-sections in the exhaust pipe plane for (a) the simulated nucleation rate (#m^{-3} s^{-1}), (b) the temperature (K), (c) mole fraction of exhaust sulphuric acid concentration and (d) CO_2 dilution ratio (148 km h^{-1}/4000 rpm).

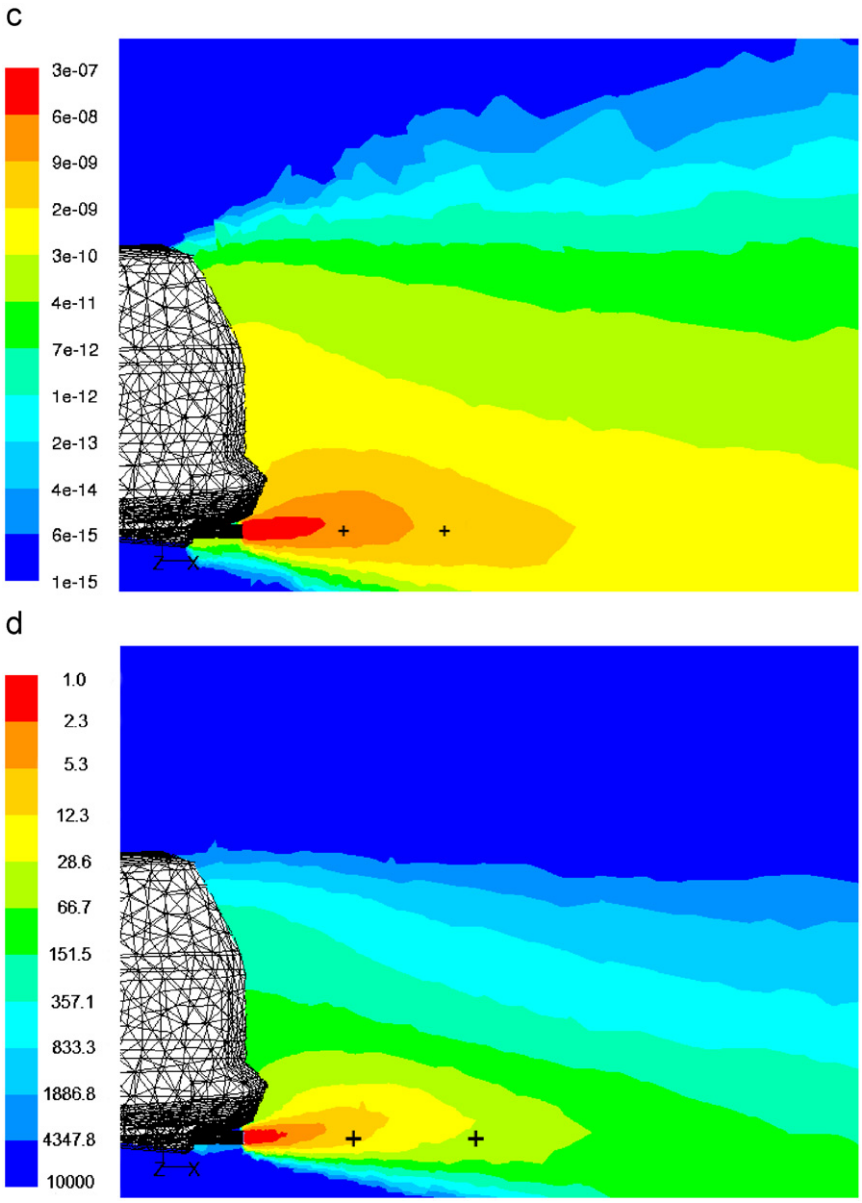

Fig. 12. (*Continued*)

concentration fluxes required in the simulations in order to generate $\sim 10^{13}\,m^{-3}$ is high. In other experiments using similar diesel engines as reported by Maricq et al. (2002), Vogt et al. (2003), Mathis et al. (2004), large nucleation particle concentrations have been reported for high load conditions and fuel sulphur contents $>320\,ppm_m$. Significant nucleation particle concentrations were recorded at $\sim 110\,km\,h^{-1}$ (Maricq et al., 2002) and $\sim 120\,km\,h^{-1}/>3000\,rpm$ (Vogt et al., 2003). In our experiments, dominating nucleation particle concentrations were recorded under high rpm (>3800) and high speed $>140\,km\,h^{-1}$. Maricq et al. (2002) analysed the catalyst oxidation efficiency for hydrocarbons, CO and SO_2 in a laboratory flow reactor. At a threshold temperature of about 160 °C, all SO_2 was converted to SO_3. They further showed that this threshold moves to higher temperatures with lower precious metal loading and aging of the catalyst.

When the fuel sulphur content is low and the vehicle is operated under high load, lube oil can become a relevant additional source for exhaust $H_2SO_{4(g)}$ due to its high sulphur content. The lube oil consumption is increased in the engine and especially at the turbo charger. Assuming a lube oil consumption of 1/1000 of fuel consumption and a lube oil sulphur content of 6000 ppm_m, lube oil can make up to 6 ppm_m fuel equivalent (Mathis et al., 2004). The high engine load conditions may further increase the lube oil consumption. In addition, purging of stored sulphur and further oxidation may occur at high catalyst temperatures of about 500 °C (Maricq et al., 2002).

Therefore, for a car running with diesel fuel with low fuel sulphur content, the simulation results suggest that the measured nucleation particle concentration may be explained by high engine load car operating conditions. At these operating conditions, exhaust sulphuric acid concentrations can be enhanced due to (i) higher sulphur–sulphate conversion rates at the catalyst related to higher exhaust temperature, (ii) release of stored sulphate on catalyst and other surfaces formed at less extreme conditions (Maricq et al., 2002; Casati et al., 2004), and (iii) a higher fuel and lube oil consumption rate. Particle size distribution measurements made at busy urban roads indicate a significant nucleation mode (Wehner et al., 2004). In urban traffic strong accelerations at, e.g., traffic lights or driving uphill may also lead to high rpm and exhaust temperature, large air mass flow and consequently purging of stored sulphate which may lead to increased new particle formation.

Laboratory experiments with dilution devices indicate a strong impact of dilution air temperature and humidity on nucleation particles. Hence, ambient temperatures may have influenced the number concentrations. Kittelson et al. (2004) found higher number concentrations related to lower ambient temperature. However, these measurements were affected by a gasoline-dominated vehicle fleet. In our simulation, ambient humidity was set to the measured relative humidity, RH, of 65%. However, due to limitations in the parameterisations used (temperature range 300–400 K), the model ambient temperature was set to 300 K, which is ~15 K higher than the measured one. Extrapolating the parameterisation beyond the validated range requires $\sim 3 \times 10^{-7}$ mol s^{-1} $H_2SO_{4(g)}$ exhaust flux to obtain number concentrations (at $x = 0.45$ m, 4×10^{13} m^{-3} and at $x = 0.9$ m, 2×10^{13} m^{-3}) similar to measured ones (~ an fsc of 10 ppm_m and a conversion rate of 0.33).

It has been reported that the classical binary H_2SO_4–H_2O nucleation theory underestimates the observed formation of nucleation mode particles by several orders of magnitude and thus further species are suspected to be involved in nucleation (Shi and Harrison, 1999; Khalek et al., 2000). Kim et al. (2002) suggested that HNO_3 can act as a precursor in low sulphur fuel. Other authors suggested that similar to the proposed ternary atmospheric nucleation (Kulmala et al., 1998, 2000; Napari et al., 2002), ammonia can increase nucleation rates due to its significant presence in gasoline exhaust gas. Mathis et al. (2004) investigated the role of organic vapours in dilution air of diesel exhaust using a fuel with >300 ppm_m sulphur content. Organic compounds such as toluene and alcohols increased the number of nucleation particles formed. Our simulation results using binary H_2SO_4–H_2O theories indicate a strong sensitivity of particle formation to sulphuric acid concentrations. Given the measurement conditions at which dominant nucleation particle concentrations were recorded, we conclude that in addition to strong mixing and high conversion rates, additional sulphur contributions from lube oil and purging of stored sulphur are required to obtain an approximate accordance between measured and simulated nucleation particle number concentrations.

4.3. Growth of nucleation particles

For H_2SO_4–H_2O nucleation particles, the simulated growth throughout the exhaust plume was lower than measured rates. Simulated nucleation particles grew to about 2.5 nm in diameter, far lower than the detection limit of the SMPS system (7 nm). Soot mode particles increased only about ~0.2 nm in diameter. Three control simulations were run where (i) the Kelvin effect was neglected using the parameterisation Eq. (A.1), (ii) the $H_2SO_{4(g)}$ mass flux was increased, and (iii) the $H_2SO_{4(g)}$ mass flux was increased and the nucleation rate was reduced by a linear factor (= 0.001). For the given model configuration, we found that neglecting the Kelvin effect did not result in significantly increased growth of nucleation particles. Increasing $H_2SO_{4(g)}$ did not result in detectable particles since the nucleation rate is highly sensitive to changes in the $H_2SO_{4(g)}$ flux leading to larger concentrations of particles too

small to detect. However, case (iii) increased $H_2SO_{4(g)}$ fluxes and reduced nucleation rates, resulted in significant growth of nucleation particles. Hence, the reason that nucleation particles do not grow sufficiently is mainly due to the small mass of condensable vapour available and to the strong condensational sink of soot mode particles. This finding is consistent with Khalek et al. (2000). Their results indicated that there is not enough H_2SO_4 vapour in the exhaust to explain observed growth. It should be noted that the number of parameters affecting nucleation and growth is large. The $H_2SO_{4(g)}$ saturation is affected by dilution, temperature, and number and size of nucleation and soot particles. Interaction with the exhaust plume water concentration also affects the nucleation rate.

Kim et al. (2002) obtained in their truck wind tunnel simulations particles growing up to ~100 nm diameter for a fuel with 125 ppm_m and a conversion rate of 0.04. However, in their work, the presence of soot mode particles was not taken into account and CFD and the aerosol model were not fully coupled.

As indicated by several other studies on heavy duty diesel engines, condensation of low and semi-volatile hydrocarbons may explain sufficient growth (Khalek et al., 2000) and composition (Tobias et al., 2001; Sakurai et al., 2003), of nucleation particles. Sakurai et al. (2003) found that the volatile component of diesel nanoparticles is comprised of at least 95% of unburned lubricating oil. Furthermore, the organic component was comprised of carbon numbers C24–C32 which were derived entirely from unburned oil.

Two condensable hydrocarbon compounds were chosen to estimate contributions of low volatile hydrocarbons on nucleation particle growth at maximum. The aliphatic hydrocarbons octane (C_8H_{18}) and gasoil ($C_{19}H_{29}$) were used. Interactions with H_2SO_4 and H_2O were not taken into account, i.e., H_2SO_4–H_2O and hydrocarbons were treated as a two-phase liquid system as suggested by Tobias et al. (2001). Mathis et al. (2004) investigated the role of organic vapours in dilution air of diesel exhaust and aliphatic hydrocarbons turned out to have no effect on the nucleation process. For both species, thermodynamic data from the FLUENT database have been used. The exhaust gas flow was chosen to be ~40% of EU HC emission limit (0.56 $g\,km^{-1}$), the equilibrium vapour pressure was set to 10^{-10} Pa based on an estimation of Tobias et al. (2001).

Fig. 13 shows the growth of simplified H_2SO_4–H_2O–HC nucleation particles compared to H_2SO_4–H_2O nucleation particles. The growth within the exhaust plume is significantly higher for particles with hydrocarbons. Nucleation particles grow to 15 nm in the near-exhaust region compared to the binary system, where they only grow to ~2.5 nm.

These results, together with the measurements, suggest that at high exhaust temperature there could be an important combination of effects enhancing new particle formation and particle growth. First, due to the high exhaust temperature a major fraction of volatile and semi-volatile species remain in the vapour phase, unless rapid dilution in the exhaust plume occurs. Second, the large amount of condensable mass leaving the exhaust pipe leads to high supersaturations favouring nucleation and rapid growth during rapid dilution. In contrast, at lower temperatures the semi-volatile species may already condense on the solid soot-mode particles within the exhaust system.

Simulation results with additional simplified hydrocarbons showed the potential of semi-volatile hydrocarbons in nucleation particle growth. The condensational growth of octane and gas–oil hydrocarbons between the exhaust pipe exit and ~1 m distance was sufficient to grow particles to 10 nm and larger.

5. Conclusions

A physical model was developed that accounts for the effects of dilution, nucleation, condensation and coagulation on particle formation and growth in the exhaust plume of a diesel fuelled vehicle, by combining a CFD model (FLUENT) with a fully coupled aerosol model, called the Fine Particle Model (FPM). The CFD set-up was verified against measurements within the exhaust plume. For temperature, humidity and CO_2 fair agreement between measurements and simulation results was obtained. Nucleation particle concentrations and growth were predicted using binary homogenous nucleation theory and assumptions about exhaust precursor gas emissions. Exhaust soot mode particle emission factors were determined based on plume measurements at 0.45 and 0.9 m. Two steady state conditions were modelled, one representing dominating soot mode concentrations as predominantly found in our measurements at medium motorway engine load conditions (120 $km\,h^{-1}$/2600 rpm).

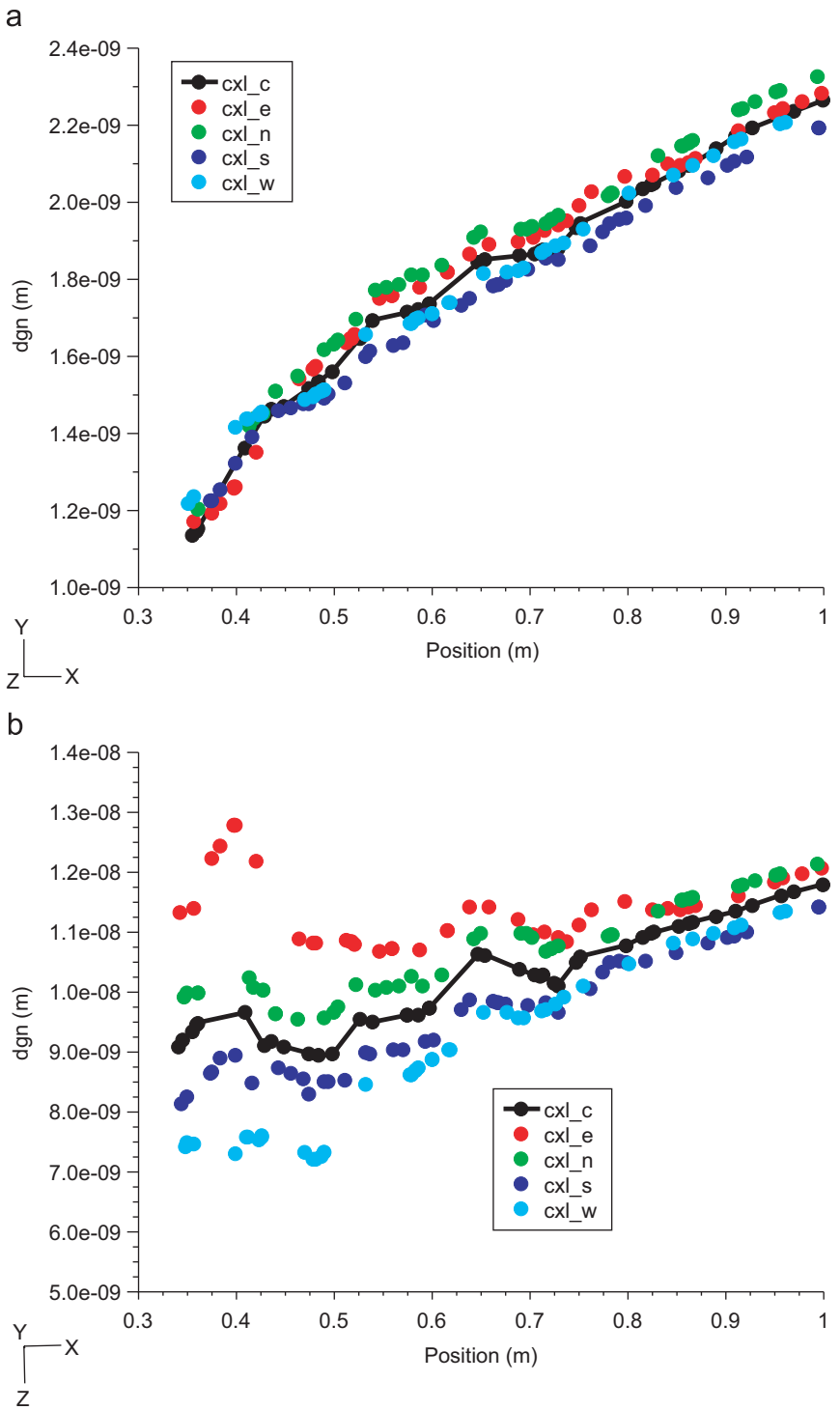

Fig. 13. Simulated d_{gn} (in m) within the near-exhaust plume region for nucleation particles consisting of H_2SO_4–H_2O (top) and simplified H_2SO_4–H_2O–HC (148 km h^{-1}/4000 rpm). Measured values ranged from 6 to 10 nm at $x = 0.45$ m, and from 11 to 16 nm at $x = 0.9$ m. Note the different scale on the y-axis.

The other represented high load test car operating conditions (148 km h^{-1}/4000 rpm) under which high nucleation particle concentrations $>10^{13}\,m^{-3}$ were measured.

The simulations revealed the importance of an accurate description of turbulent species and particle transport. Rapid dispersion of soot mode particles is the dominating process to explain the measured decrease of soot mode number concentrations between 0.45 and 0.9 m behind the exhaust pipe. The impact of coagulation on soot mode number concentrations was negligible. A soot mode emission factor of $2.1\times10^{14}\,km^{-1}$ was determined based on our measurements for conditions representing 120 km h^{-1} and 2600 rpm, $2.6\times10^{14}\,km^{-1}$ for conditions representing 148 km h^{-1} and 4000 rpm.

Simulations for 148 km h^{-1}/4000 rpm showed a strong sensitivity of nucleation mode particles to prescribed $H_2SO_{4(g)}$ exhaust fluxes: 9×10^{-7} mol s^{-1} resulted in up to $2\times10^{13}\,m^{-3}$ at 0.45 m and $1\times10^{13}\,m^{-3}$ at 0.9 m distance behind the exhaust pipe. This $H_2SO_{4(g)}$ exhaust flux corresponds to a fuel sulphur content of 10 ppm_m and a conversion rate of 1 at $T=300$ K. Highest nucleation rates are located where gradients of temperature, humidity and $H_2SO_{4(g)}$ are strongest and dilution gradients as indicated by CO_2 are strongest.

In contrast to other measurements, the test car was run with ultra low sulphur fuel (<10 ppm_m), which has been the most common diesel fuel in Germany since 2005. Our results based on measurements and simulations suggest that large nucleation particle number concentrations are related to strong dilution gradients, high SO_2 to SO_3 conversion rates and additional sulphur contributions from lube oil and purging of stored sulphur at high engine load conditions.

For the prescribed $H_2SO_{4(g)}$ exhaust flux, the simulated growth of H_2SO_4–H_2O particles was unrealistically low to explain measured nucleation particle concentrations. The reason for the simulated insufficient growth is the limited condensable H_2SO_4–H_2O vapour mass opposed to the strong additional condensational sink of soot mode particles. Hence, other low and semi-volatile condensable species such as hydrocarbons are required to explain size and number concentrations of measured nucleation particles.

Simulation results with additional simplified low and semi-volatile hydrocarbons suggest that the growth of nucleation mode particles within close distance (~1 m) from the exhaust pipe could be caused by organic species with very low vapour pressures.

Our simulation results are limited with respect to exact boundary conditions and complex engine and exhaust aftertreatment thermodynamics affecting the emissions of volatile species. Additional motor test-bed measurements (e.g. HC or even H_2SO_4) and measurements at the catalyst (e.g. catalyst temperature) may provide further important information. Combined CFD and aerosol model simulations may be used for the design of exhaust aftertreatment devices and their impact on, e.g., nucleation or diffusion loss due to wall adsorption in the near future.

Acknowledgements

This project was funded by the German Research Council (DFG). Technical support by Martin Wilck from Particle-Dynamics is highly acknowledged. We thank Ulf Kirchner (Ford Research Centre Aachen), Thomas Beckmann (Daimler-Chrysler) and Michael Zallinger (TU-Graz) for interesting and helpful discussions.

Appendix

Mole fraction parameterisations

To save computing time, we developed a parameterisation for the sulphuric acid mole fraction x in water solution which results in a set relative humidity, RH, in the equilibrium vapour over solution surface. Separate parameterisations were developed for the flat surface case and for the solution droplet with radius r.

For the flat surface case, the equation giving the mole fraction equilibrium is

$$\mathrm{RH} = A_{\mathrm{l,w}}(x, T),$$

where $A_{\mathrm{l,w}}$ is the experimentally based liquid phase activity of water for sulphuric acid solution and T is temperature. We used values for the liquid phase activity from Zeleznik (1991).

For the spherical droplet with radius r, the equation RH can be expressed as

$$\mathrm{RH} = A_{\mathrm{l,w}}(x, T)\,\exp\left(\frac{2\sigma(x, T)v_{\mathrm{w}}(x, T)}{rkT}\right),$$

where k is the Boltzmann constant, σ is the surface tension of the solution, v_{w} is the partial molecular

volume of water in the solution calculated from liquid density ρ_l as $v_w \equiv \partial[(N_w \times m_w + N_a \times m_a)/\rho_l(x)]/\partial N_w$, where m_w and m_a are the molecular weights of water and acid, respectively, and N_w and N_a are the number of molecules in the solution with mole fraction $x = N_a/(N_a + N_w)$. We used the surface tension parameterisation by Vehkamäki et al. (2003) and liquid density parameterisation by Vehkamäki et al. (2002).

The parameterisation for a flat surface case is

$$x(\mathrm{RH}, T) = \frac{a + bT + c\,\ln rh + d\,\ln(rh)^2 + e\,\ln(rh)^3}{100[1 + fT + g\,\ln rh + h\,\ln(rh)^2 + i\,\ln(rh)^3]},$$

where $rh = \mathrm{RH}/100\%$ and RH is expressed in %, and temperature T is in K.

For spherical droplets, the parameterisation is

$$x(\mathrm{RH}, T) = \frac{a + bT + c\,\ln rh + d\,\ln(rh)^2 + e\,\ln(rh)^3}{100[1 + fT + g\,\ln rh + h\,\ln(rh)^2 + i\,\ln(rh)^3]} \quad (A.1)$$

with r in nm, and

$$A(T, r) = a(T) + b(T)\ln r + c(T)(\ln r)^2. \quad (A.2)$$

The coefficients a–i for both flat and spherical surfaces are listed in Table A.1.

The parameterisations are valid for temperatures from 300 to 400 K, relative humidities from 1% to 95%, and droplet radii from 1 to 100 nm. Results are shown in Figs. A.1 and A.2.

For the flat surface parameterisation, x_{param}/x varies from 0.89 and 1.38, and for the spherical droplet case $0.86 < x_{\mathrm{param}}/x < 1.28$.

Table A.1
Coefficients for the parameterisations, T in Kelvin

	Flat surface	Spherical droplet
a	3.2199	$0.4794 + 0.099447T - 1.7216 \times 10^{-4}T^2$
b	-6.9520×10^{-3}	$7.1139 - 0.089509T + 1.4410 \times 10^{-4}T^2$
c	−10.001	$-1.3638 + 0.014502T - 2.3250 \times 10^{-5}T^2$
d	−2.4238	$81.732 - 0.63790T + 9.4502 \times 10^{-4}T^2$
e	−0.31948	$-68.475 + 0.45440T - 7.0104 \times 10^{-4}T^2$
f	-1.5973×10^{-3}	$-0.19267 + 1.5054 \times 10^{-3}T - 2.6675 \times 10^{-6}T^2$
g	−0.10600	$5.9169 - 0.044958T + 7.3156 \times 10^{-5}T^2$
h	-4.6853×210^{-2}	–
i	-6.9268×10^{-3}	–

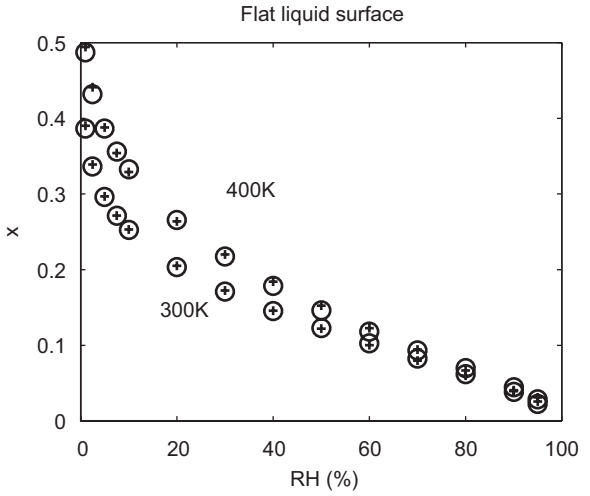

Fig. A.1. Equilibrium mole fractions (plus signs) and values produced by the parameterisation (circles) as a function of relative humidity at temperatures of 300 and 400 K (flat surface).

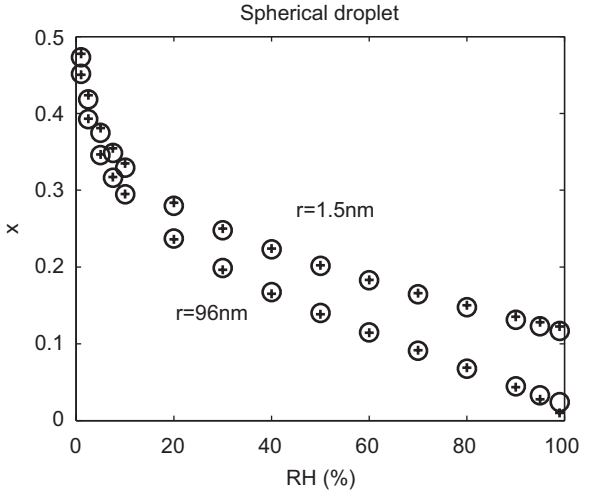

Fig. A.2. Equilibrium mole fractions (plus signs) and values produced by the parameterisation (circles) as a function of relative humidity for droplet radii of 15 and 96 nm at an exhaust temperature of 360 K.

References

Baumgard, K.J., Johnson, J.H., 1996. The effect of fuel and engine design on diesel exhaust particle size distributions, SAE 960131. pp. 37–50.

Berndt, T., Böge, O., Stratmann, F., Heintzenberg, J., Kulmala, M., 2005. Rapid formation of sulfuric acid particles at near-atmospheric conditions. Science 307 (5710), 698–700.

Casati, R., Scheer, V., Kirchner, U., Benter, T., Vogt, R., 2004. Particle size distributions in diesel exhaust under ambient and

laboratory dilution conditions. In: Proceedings of the Eighth ETH Conference on Combustion Generated Nanoparticles.

DECSE, 1999. Phase I Interim Data Report No. 3: Diesel Fuel Sulfur Effects on Particulate Matter Emissions, US Department of Energy.

Donaldson, K., Li, X.Y., MacNee, W., 1998. Ultrafine (nanometre) particle mediated lung injury. Journal of Aerosol Science 29, 553–560.

Giechaskiel, B., Ntziachristos, L., Samaras, Z., Scheer, V., Casati, R., Vogt, R., 2005. Formation potential of vehicle exhaust nucleation mode particles on-road and in the laboratory. Atmospheric Environment 39, 3191–3198.

Harris, S.J., Maricq, M.M., 2001. Signature size distributions for diesel and gasoline engine exhaust particulate matter. Journal of Aerosol Science 32, 749–764.

Jacobson, M.Z., 2002. Control of fossil-fuel particulate black carbon and organic matter, possibly the most effective method of slowing global warming. Journal of Geophysical Research 107 (D19), 4410.

Jiang, P., Lignell, D.O., Kelly, K., Lighty, J.S., Sarofim, A.F., Montgomery, C.J., 2005. Simulation of the evolution of particle size distributions in a vehicle exhaust plume with unconfined dilution by ambient air. Journal of the Air & Waste Management Association 55 (4).

Khalek, I.A., Kittelson, D.B., Brear, F., 1999. The influence of dilution conditions on diesel exhaust particle size distribution measurements, SAE 1999-01-1142.

Khalek, I.A., Kittelson, D.B., Brear, F., 2000. Nanoparticle growth during dilution and cooling of diesel exhaust: experimental investigation and theoretical assessment, SAE-2000-01-0515.

Kim, D.-H., Gautam, M., Gera, M., 2001. On the prediction of concentration variations in a dispersing heavy-duty truck exhaust plume using k–ε turbulent closure. Atmospheric Environment 25, 5267–5275.

Kim, D.-H., Gautam, M., Gera, M., 2002. Parametric studies on the formation of diesel particulate matter via nucleation and coagulation modes. Journal of Aerosol Science 33, 1609–1621.

Kittelson, D.B., 1998. Engines and nanoparticles: a review. Journal of Aerosol Science 29, 575–588.

Kittelson, D.B., Watts, W.F., Johnson, J.P., 2004. Nanoparticle emissions on Minnesota highways. Atmospheric Environment 38, 9–19.

Kulmala, M., Laaksonen, A., Pirjola, L., 1998. Parameterisations for sulphuric acid/water nucleation rates. Journal of Geophysical Research 103, 8301–8307.

Kulmala, M., Pirjola, L., Mäkelä, J.M., 2000. Stable sulphate clusters as a source of new atmospheric particles. Nature 404, 66–69.

Maricq, M.M., Chase, R.E., Xu, N., Laing, P., 2002. The effects of the catalytic converter and fuel sulfur level on motor vehicle particulate matter emissions: light duty diesel vehicles. Environmental Science and Technology 36, 283–289.

Mathis, U., Mohr, M., Zenobi, R., 2004. Effect of organic compounds on nanoparticles formation in diluted diesel exhaust. Atmospheric Chemistry and Physics 4, 609–620.

Napari, I., Noppel, M., Vehkamäki, H., Kulmala, M., 2002. Parameterization of ternary nucleation rates for H_2SO_4–NH_3–H_2O vapors. Journal of Geophysical Research 107 (D19), 4318.

Penner, J.E., Zhang, S.Y., Chuang, C.C., 2003. Soot and smoke aerosol may not warm climate. Journal of Geophysical Research 108 (D21), 4657.

Peters, A., Wichmann, H.E., Tuch, Th., Heinrich, J., Heyder, J., 1997. Respiratory effects are associated with the number of ultrafine particles. American Journal of Respiratory and Critical Care Medicine 155, 1376–1383.

Peters, A., Dockery, D., Muller, J.E., Mittleman, M.A., 2001. Increased particulate air pollution and the triggering of myocardinal infarction. Circulation 103, 2810–2815.

Pope, C.A., 2000. What do epidemiologic findings tell us about heath effects of environmental aerosols? Journal of Aerosol Medicine 1314, 335–354.

Sakurai, H., Tobias, H.J., Park, K., Zarling, D., Docherty, S., Kittelson, D.B., McMurry, P.H., Ziemann, P.J., 2003. On-line measurements of diesel nanoparticles composition and volatility. Atmospheric Environment 37, 1199–1210.

Scheer, V., Kirchner, U., Casati, R., Vogt, R., Wehner, B., Philippin, S., Wiedensohler, A., Hock, N., Schneider, J., Weimer, S., Borrmann, S., 2005. Composition of semi-volatile particles from diesel exhaust, SAE 2005-01-0197.

Shi, J.P., Harrison, R.M., 1999. Investigation of ultrafine particle formation during diesel exhaust dilution. Environmental Science and Technology 33, 3730–3736.

Somers, C.M., McCarry, B.E., Malek, F., Quinn, J.S., 2004. Science 304, 1008–1010.

Sydbom, A., Blomberg, A., Parnia, S., Stenfors, N., Sandstrom, T., Dahlen, S.E., 2001. Health effects of diesel exhaust emissions. European Respiratory Journal 17, 733–746.

Tobias, H.J., Beving, D.E., Ziemann, P.J., Sakurai, H., Zuk, M., McMurry, P.H., Zarling, D., Waytulonis, R., Kittelson, D.B., 2001. Chemical analysis of diesel engine nanoparticles using a nano-DMA/thermal desorption particle beam mass spectrometer. Environmental Science and Technology 35, 2233–2243.

Vehkamäki, H., Kulmala, M., Napari, I., Lehtinen, K.E.J., Timmreck, C., Noppel, M., Laaksonen, A., 2002. An improved parameterization for sulphuric acid-water nucleation rates for tropospheric and stratospheric conditions. Journal of Geophysical Research 107 (D22), 4622.

Vehkamäki, H., Kulmala, M., Lehtinen, K.E.J., Noppel, M., 2003. Modelling binary homogeneous nucleation of water—sulfuric acid vapurs: parameterisation for high temperature emissions. Environmental Science and Technology 37, 3392–3398.

Vogt, R., Scheer, V., Casati, R., Benter, Th., 2003. On-road measurement of particle emission in the exhaust plume of a diesel passenger car. Environmental Science and Technology 37, 4070–4076.

von Löwis, S., 2006. Measurements within the exhaust plume of passenger cars under real atmospheric dilution and on-road driving conditions. Dissertation, Universität Leipzig.

Wehner, B., 2000. Particle formation in the urban atmosphere. Dissertation, Universität Leipzig.

Wehner, B., Philippin, S., Wiedensohler, A., Scheer, V., Vogt, R., 2004. Variability of non-volatile fractions of atmospheric aerosol particles with traffic influence. Atmospheric Environment 38, 6081–6090.

Whitby, K.T., 1978. The physical characteristics of sulfur aerosols. Atmospheric Environment 12, 135–159.

Wilck, M., 1998. Modal modelling of multicomponent aerosols. Dissertation, Universität Leipzig.
Wilck, M., Stratmann, F., 1997. A 2-D multicomponent modal aerosol model and its application to laminar flow reactors. Journal of Aerosol Science 28, 959–972.
Yu, F., 2001. Chemiions and nanoparticles formation in diesel engine exhaust. Geophysical Research Letters 28, 4191–4194.
Zeleznik, F.J., 1991. Thermodynamic properties of the aqueous sulphuric system to 350 K. Journal of Physical and Chemical Reference Data 20, 1157–1200.